AMERICAN SOCIETY FOR MICROBIOLOGY | Antimicrobial Agents and Chemotherapy

Virology | Full-Length Text

Pan-antiviral effects of a PIKfyve inhibitor on respiratory virus infection in human nasal epithelium and mice

Jonathan Baker,[1] Hugo Ombredane,[1] Leah Daly,[1] Ian Knowles,[2] Garth Rapeport,[1] Kazuhiro Ito[1]

AUTHOR AFFILIATIONS See affiliation list on p. 13.

ABSTRACT Endocytosis, or internalization through endosomes, is a major cell entry mechanism used by respiratory viruses. Phosphoinositide 5-kinase (PIKfyve) is a critical enzyme for the synthesis of phosphatidylinositol (3, 5)biphosphate (PtdIns (3, 5)P2) and has been implicated in virus trafficking *via* the endocytic pathway. In fact, antiviral effects of PIKfyve inhibitors against SARS-CoV-2 and Ebola have been reported, but there is little evidence regarding other respiratory viruses. In this study, we demonstrated the antiviral effects of PIKfyve inhibitors on influenza virus and respiratory syncytial virus *in vitro* and *in vivo*. PIKfyve inhibitors Apilimod mesylate (AM) and YM201636 concentration-dependently inhibited several influenza strains in an MDCK cell-cytopathic assay. AM also reduced the viral load and cytokine release, while improving the cell integrity of human nasal air-liquid interface cultured epithelium infected with influenza PR8. In PR8-infected mice, AM (2 mg/mL), when intranasally treated, exhibited a significant reduction of viral load and inflammation and inhibited weight loss caused by influenza infection, with effects being similar to oral oseltamivir (10 mg/kg). In addition, AM demonstrated antiviral effects in RSV A2-infected human nasal epithelium *in vitro* and mouse *in vivo*, with an equivalent effect to that of ribavirin. AM also showed antiviral effects against human rhinovirus and seasonal coronavirus *in vitro*. Thus, PIKfyve is found to be involved in influenza and RSV infection, and PIKfyve inhibitor is a promising molecule for a pan-viral approach against respiratory viruses.

KEYWORDS Apilimod, PIKfyve, influenza, respiratory syncytial virus, human rhinovirus, coronavirus, air-liquid interface

Respiratory virus infections cause an enormous disease burden both in children and in adults throughout the world. Influenza A and B viruses, respiratory syncytial virus (RSV), as well as SARS-CoV-2 are responsible for the highest numbers of deaths and hospitalizations worldwide, but other respiratory viruses, including rhinovirus, parainfluenza viruses, adenovirus, human bocavirus, and seasonal coronaviruses, are also currently known to cause severe diseases in addition to mild upper respiratory tract infections, especially in patients with chronic respiratory diseases (1, 2). It is now recognized that virus-induced exacerbations are preventable through COVID-19 pandemic experiences (3). To tackle respiratory virus infection, the one-target-one-drug-paradigm approach is usually taken, which is characterized by many failures and great uncertainty. Especially, the initiation of the treatment requires an appropriate diagnosis of the specific virus, or prophylaxis treatment is difficult without the prediction of particulate virus infection. Particularly, to prepare for unforeseen pandemics or protect from several respiratory viruses, a pan-viral approach is more attractive.

The endosome/lysosome system is crucial for the activity-dependent internalization of membrane proteins and contributes to the regulation of lipid levels on the plasma membrane (4). Some viruses hijacked this route to deliver their genome into cells for replications (5). Phosphatidylinositol 3-phosphate 5-kinase (PIKfyve) is

Editor Miguel Angel Martinez, IrsiCaixa Institut de Recerca de la Sida, Badalona, Barcelona, Spain

Address correspondence to Kazuhiro Ito, k.ito@imperial.ac.uk.

J. Baker and H. Ombredane received the research funding from SubIntro Ltd. K. Ito and G. Rapeport were co-founders of SubIntro Ltd. and former consultants of the company. Other authors declare no conflict of interest.

See the funding table on p. 14.

Received 11 August 2023
Accepted 6 November 2023
Published 8 December 2023

a phosphoinositide 5-kinase that phosphorylates phosphatidylinositol-3-phosphate (PI (3)P), synthesizing PtdIns5P and PtdIns (3, 5) biphosphate, which, in turn, regulates endomembrane homeostasis. In fact, PIKfyve is reported to be involved in the entry of viruses into host cells, including the Ebola virus, the Marburg virus, and SARS-CoV-2 (6).

Apilimod mesylate (AM) is a well-known PIKfyve inhibitor with a sub-nano molar potency, originally developed for the treatment of Crohn's disease and rheumatoid arthritis due to inhibitory activities of interleukins 12 and 23 production (7, 8). However, the clinical trials' results were disappointing, and the development of Apilimod for this application was halted, mainly due to poor pharmacokinetics (unexpected low plasma concentration and poor bioavailability) (9, 10). PIKfyve inhibitors have recently been re-discovered as potential antiviral agents against filovirus and SASR-CoV-2 (6, 11–13). The inhibitor is also reported to disrupt the entry or replication of RNA viruses broadly, including enterovirus, coxsackievirus B3, poliovirus, Zika virus, and vesicular stomatitis virus (14). AM is reported to impair SARS-CoV-2 entry into mammalian cell lines and potentially suppress viral replication (13, 15). The results of a clinical trial against COVID-19 (NCT04446377) are not yet available, but until improved pharmacokinetics are achieved, an issue with use possibly remains. In this report, to overcome these problems, the potential of intranasal route delivery was explored rather than oral treatment.

Historically, virus infection research was conducted using submerged culture monolayer (2D) cancer lines which are susceptible to specific virus species. However, especially through the COVID-19 pandemic, it was realized that positive outcomes from cancer cell lines were not necessarily translational to the clinic. Air-liquid interface (ALI) cultured airway epithelium are being increasingly recognized for their ability to overcome many of the disadvantages of submerged cell culture models (16–18). It consists of pseudostratified fully differentiated cells cultured in transwell inserts, wherein the apical cells are exposed to the air and the basolateral cells submerged in a culture medium, and thus a more structurally and biologically accurate representation of the human respiratory microenvironment. Attempts to repurpose existing drugs for SARS-CoV-2 treatment identified the anti-malaria drug chloroquine, which demonstrated potent antiviral activity against SARS-CoV-2 in a submerged cancer cell culture model (Vero E6 cells) (19). However, it was later proved to have limited efficacy in clinical trials and was confirmed to have unsuccessfully reduced SARS-CoV-2 infection in ALI tissue culture models (20–22), perhaps indicating that these ALI models more accurately simulate human airway tissue responses. In addition, virus replication kinetics observed in ALI airway epithelium are similar to the outcomes from human challenge studies with SARS-CoV-2, influenza, and RSV (23–26). Furthermore, we can mimic intranasal treatment using ALI two-chamber systems, by applying compounds apically.

Thus, the aim of this study is to investigate the pan-viral potentials of AM using influenza and RSV-infected ALI-cultured airway epithelium *in vitro* and mice *in vivo* by intranasal route. The antiviral effects of AM against human rhinovirus and seasonal coronaviruses were also evaluated *in vitro*.

RESULTS

Anti-viral profiles of PIKfyve inhibitors against respiratory virus panel

First, the antiviral activities of PIKfyve inhibitors Apilimod and YM201636 were assessed in *in vitro* cytopathic effect (CPE) assays in MDCK cells against influenza strains including pandemic, amantadine resistant, or oseltamivir resistant. AM potently inhibited CPE induced by influenza (H1N1, H3N2, H5N1, influenza B) with IC_{50} ranged from 3.8 to 24.6 µM with E-max of 100% (Table 1; Fig. 1). AM did not affect cell viability at the concentrations up to 54 µM, and consequently showed a large safety margin with respect to mammalian cell toxicity (Table 1; Fig. 1). The inhibitory effects of AM were similar to or more potent than those of known antiviral, ribavirin (Table 1). In addition, another PIKfyve inhibitor, YM201636 showed potent antiviral effects against H1N1 A/California/07/2006, H3N2 Perth/16/2009and H5N1 Duck/MN/12525/81, suggesting a potential class effect. However, YM201636 did not inhibit influenza B at all

TABLE 1 Antiviral effects of PIKfyve inhibitors against influenza isolates in MDCK cells, evaluated by CPE[a]

Virus strain		Apilimod mesylate				YM201636				Ribavirin			
		IC_{50} (μM)	IC_{90} (μM)	CC_{50} (μM)	SI	IC_{50} (μM)	IC_{90} (μM)	CC_{50} (μM)	SI	IC_{50} (μM)	IC_{90} (μM)	CC_{50} (μM)	SI
H1N1	A/California/07/2009 (exp1)	9.5	27.8	>54	>5.7	3.0	21.4	>21.4	>7.1	11.1			
H1N1	A/California/07/2009 (exp 2)	9.2	31.1	>54	>5.9	–[b]	–	–	–	25.0	221.1	>4095	>164
H1N1	A/Hong Kong/2369/2009	6.1	22.9	>54	>8.9	–	–	–	–	28.7	151.5	>4095	>143
H1N1	A/Massachusetts/15/2013	10.8	31.1	>54	>5.0	–	–	–	–	21.7	118.8	>4095	>189
H1N1	A/Louisiana/08/2013	6.7	29.5	>54	>8.0	–	–	–	–	29.5	176.1	>4095	>139
H1N1	A/Pennsylvania/30/2009	24.6	47.5	>54	>2.2	–	–	–	–	24.6	139.2	>4095	>167
H1N1	A/Michigan/45/2015	10.6	34.4	>54	>5.1	–	–	–	–	24.6	86.0	>4095	>167
H3N2	A/Ohio/88/2012v(H3N2)	3.8	18.0	>54	>14	–	–	–	–	15.6	86.0	>4095	>263
H3N2	Perth/16/2009	5.1	19.6	>54	>11	0.7	3.4	>21.4	>29	4.9	32.3	7272	1480
H5N1	Duck/MN/1525/81	4.7	19.6	>54	>11	5.6	14.8	>21.4	>3.8	13.5	73.7	6220	460
FluB	Florida/4/2006	16.4	47.5	>54	>3.3	>21.4	>21.4	>21.4	ND	6.1	33.6	6220	1013

[a]IC_{50} IC_{90} = concentration required for 50% and 90% inhibition, respectively, CC_{50} = concentration to show 50% of cell death, SI: safety index = CC_{50}/IC_{50}.
[b] "–": not done.

concentrations up to 21.4 μM. As the highest concentration was found not to be toxic, further testing at higher concentrations will be required to confirm the result.

AM and YM also exhibited potent inhibition of CPE induced by seasonal coronavirus (229E, OC43) and human rhinovirus (HRV14 and HRV1B), and particularly, the effects against seasonal CoV were very potent (Table 2). The effects of AM against RSV A2 and PIV-3 were inconclusive as they produced cell toxicity in cells used for this assay (MA104 cells, an epithelial cell line from the kidney of an African green monkey). YM did not inhibit the replication of RSV A2 and PIV3 up to 21 μM (Table 2). As the concentration did not show the cell toxicity, it is inconclusive until higher concentrations are tested.

Effects of AM on H1N1 infection in ALI-cultured human nasal epithelium

The antiviral effects of AM were also evaluated using ALI-cultured fully differentiated human primary nasal epithelium. Following inoculation with a low level of influenza PR8 strain (0.02 MOI), the quantity of virus in apical washes, as determined by $TCID_{50}$ assay, increased from Day 1 to a peak at Days 1–2 followed by a modest reduction on Day 3 (Fig. 2A). We also found that the viral load waned gradually and modestly up to Day 7 (data not shown). Treatment with AM to the apical surface, once daily from Day 0 (10 min before and 60 min together with virus inoculum) to Day 1 (15-min exposure only), induced a concentration-dependent inhibition of H1N1 virus release on Day 2 post-virus inoculation, and the effect of 0.2 mg/mL AM was statistically significant (Fig. 2B). In a separate experiment, we found the effects of AM 2 mg/mL were similar to that with Oseltamivir carboxylate 0.2 mg/mL (Table 3).

H1N1 infection modestly reduced cell integrity determined as TEER (*trans* epithelial electrical conduct) on Day 1 post-inoculation, and then gradually increased (Fig. 2C). The level of TEER was also restored by apical AM treatment at 0.2 mg/mL, although it is not statistically significant (Fig. 2D). H1N1 infection also caused RANTES and CXCL8 production in the apical surface, determined in apical washes. Both peaked on Day 2 post-virus inoculation (Fig. 2E). AM 0.2 mg/mL statistically significantly inhibited the release of RANTES and CXCL8 on Day 2 post-inoculation (Fig. 2F and G).

Effects of Apilimod mesylate on H1N1 infection in mice *in vivo*

Once daily treatment with Apilimod base (AB: 0.5, 2 mg/mL) in phosphate-buffered saline (PBS) with 10% dimethyl sulfoxide (DMSO), on days 0 to 3, by intranasal (i.n.) administration, was found to inhibit body weight loss by PR8 influenza virus infection in BALB/c mice where oral treatment oseltamivir 10 mg/kg demonstrated marked protection (Fig. 3A). The effects of AM dissolved in water at 2 mg/mL (40 μg/mouse [approx. 1.6 mg/kg)]) showed similar protective effects against body weight loss (Fig. 3B).

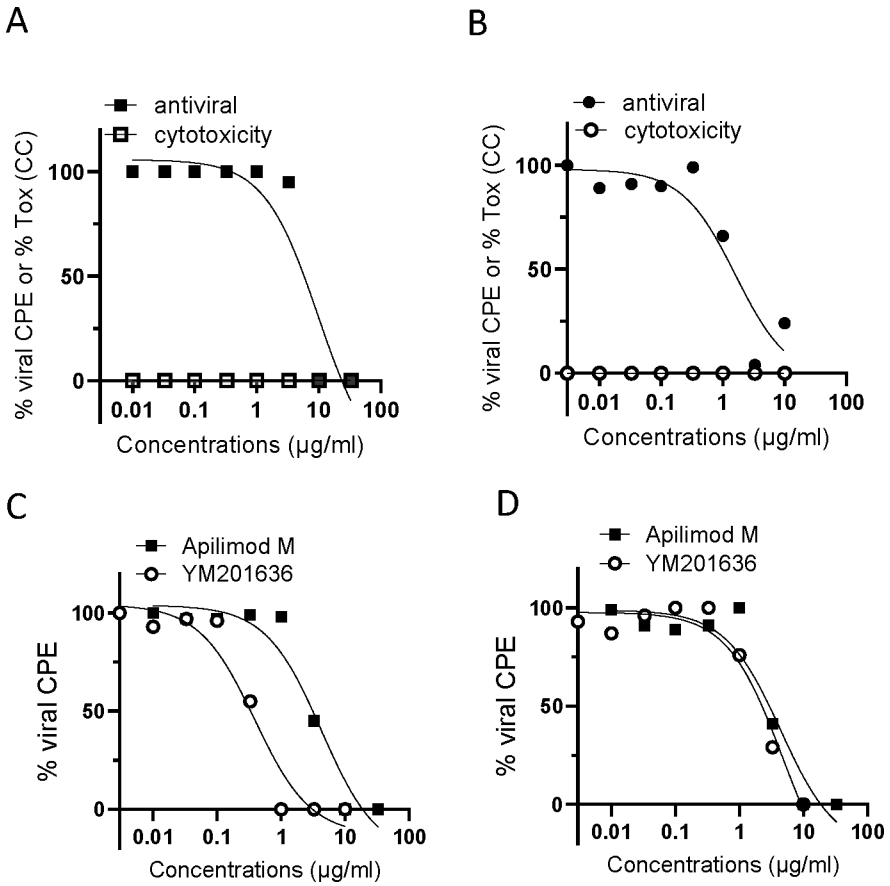

FIG 1 Antiviral effects of PIKfyve inhibitors against influenza isolates. (A) Concentration-dependent cell toxicity and antiviral effects of apilimod mesylate (AM) in MDCK cells infected with H1N1 A/California/07/2009. (B) Concentration-dependent cell toxicity and antiviral effects of YM201636 (YM) in MDCK cells infected with H1N1 A/California/07/2009. (C) Antiviral effects of AM and YM in MDCK cells infected with H3N2, A/Ohio/88/2012 v. (D) Antiviral effects of AM and YM in MDCK cells infected with H5N1, Duck/MN/1525/81. Compounds were treated at the same time when the virus was inoculated, and CPE was determined on Day 3 post-inoculation by neutral red staining.

Viral loads in the lungs of H1N1 (PR8)-infected mice were also significantly inhibited by intranasal AB and AM (both 2 mg/mL) as well as oral oseltamivir (Fig. 3C). In addition, AB at 2 mg/mL showed a significant reduction in the viral loads in the nasal tissue, although AM showed a trend of reduction (P = 0.0501) (Fig. 3D). The treatment also showed the inhibition of neutrophil and lymphocyte accumulation in nasal and lung lavage on 5 days post-virus inoculation (Table 4).

TABLE 2 Antiviral effects of PIKfyve inhibitors against other respiratory viruses[a]

Virus strain	Apilimod mesylate				YM201636					Reference			
	IC_{50} (µM)	IC_{90} (µM)	CC_{50} (µM)	SI	IC_{50} (µM)	IC_{90} (µM)	CC_{50} (µM)	SI		IC_{50} (µM)	IC_{90} (µM)	CC_{50} (µM)	SI
HRV14	12.3	40.9	>54	>4.4	7.5	23.5	>21.4	>2.9	Pirodavir	0.003	0.019	37.9	14,000
HRV1B	0.52	2.8	>54	>103	–	–	–	–	Pirodavir	0.016	0.053	40.9	2,500
hCoV-229E	0.04	0.23	>54	>1375	4.5	>21.4	>21.4	>4.8	M128533[b]	0.19	1.1	>10	>53
hCoV-OC43	0.007	0.030	1.3	193	0.9	4.1	>21.4	>25	M128533[b]	0.12	1.1	>10	>83
RSV A2	19.6	44.2	29.5	1.5	>21.4	>21.4	>21.4	–	Ribavirin	8.6	53.2	2047	238
PIV-3	31.1	52.4	18.0	0.58	>21.4	>21.4	>21.4	–	Ribavirin	73.7	356	606	8.2

[a]IC_{50} IC_{90} = concentration required for 50% and 90% inhibition, respectively, CC_{50} = concentration to show 50% of cell death. SI: safety index = CC_{50}/IC_{50}.
[b]µg/mL

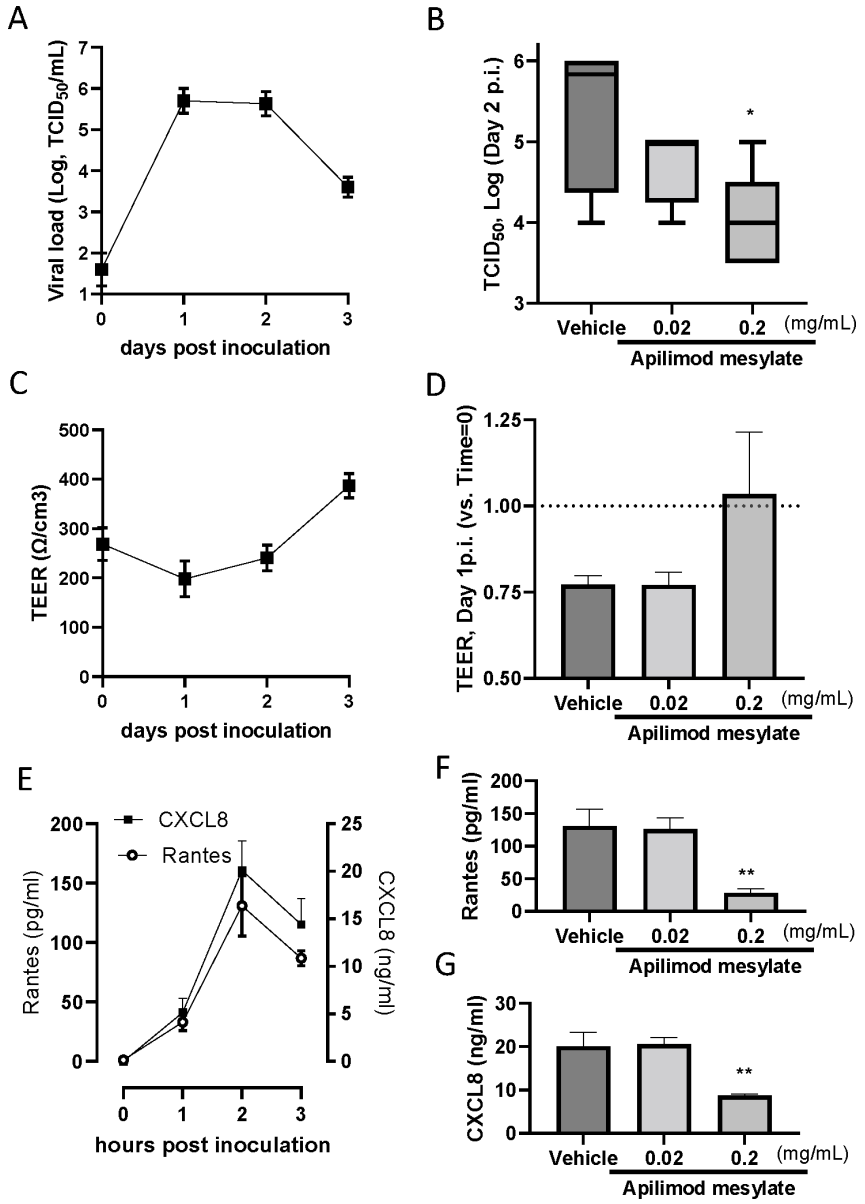

FIG 2 Effects of Apilimod mesylate on H1N1(PR8) infected ALI-cultured nasal epithelium. (A) Kinetics of H1N1 viral load in apical washes post-virus inoculation. On Day 0, the virus was inoculated and removed after 60 min of absorption. Apical washes were collected after 1-hour incubation (and wash) on Day 0, and once daily from Day 1 to Day 3. (B) Viral load determined by $TCID_{50}$ assay in apical washes from the inserts treated vehicle and AM, which were collected on Day 2 post-inoculation. (C) Kinetics of cell integrity determined as TEER post-virus inoculation. (D) TEER determined in epithelium inserts treated with vehicle and AM on Day 2 post-inoculation. (E) The kinetics of Rantes and CXCL8 release in apical washed from the epithelium inserts infected with H1N1, and the effects of AM on Rantes (F) and CXCL8 (G) in apical washes collected on Day 2 post-inoculation.

Effects of Apilimod mesylate on RSV A2 infection in ALI-cultured human nasal epithelium *in vitro* and in mice *in vivo*

The antiviral effect of AM was also evaluated using ALI-cultured fully differentiated human primary nasal epithelium infected with RSV A2. Following inoculation with a low level of RSV A2 (0.01 MOI), the quantity of RSV in apical washes, as determined by plaque assay, increased from Day 1 to Day 2 (Fig. 4A). Treatment with AM to the apical

TABLE 3 H1N1 viral load in apical wash from ALI nasal epithelium treated with Apilimod or oseltamivir

		Hour post-H1N1 inoculation (Log, pfu/mL: geometric mean ± SD, *n* = 3)	
		24 hours	48 hours
Vehicle (H_2O)	Apical	2.9 ± 0.22	3.5 ± 0.39
Apilimod mesylate (0.2 mg/mL)	Apical	2.7 ± 0.30	2.9 ± 0.32
Apilimod mesylate (2 mg/mL)	Apical	2.2 ± 0.16[b]	2.0 ± 0.14[b]
Oseltamivir carboxylate (0.2 mg/mL)	Basal	2.1 ± 0.10[b]	2.1 ± 0.20[b]

[a]Changes in each group were compared to virus-infected epithelium treated with the vehicle using Dunnett's one-way analysis of variance.
[b]$P < 0.05$.

surface, once daily from Day 0 (15 min before virus inoculation +60 min with virus) to Day 1 (30-min incubation), induced a concentration-dependent inhibition of RSV A2 replication. Particularly, the effect at a concentration of 2 mg/mL (approximately 1.5 Log

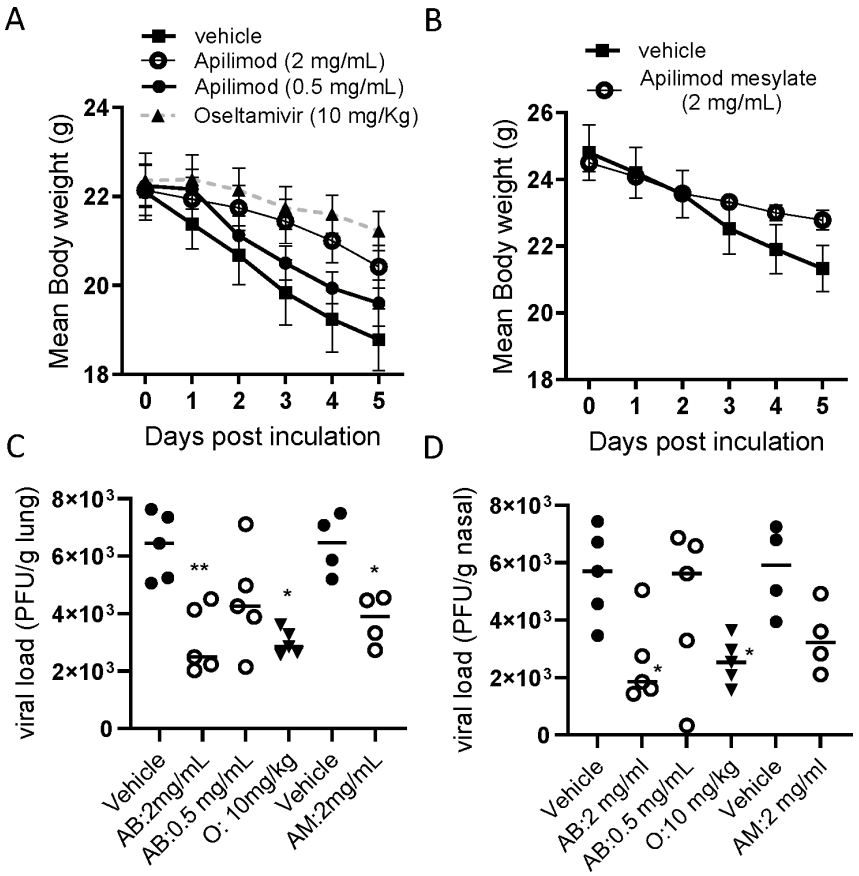

FIG 3 Effects of intranasal apilimod (Apilimod base: AB, and Apilimod mesylate: AM) treatment on H1N1-infected BALB/c mice. Mice were inoculated intranasally with H1N1 PR8 (1.0×10^5 PFU/mouse), and the animals were sacrificed 5 days post-virus inoculation. Apilimod was treated once daily on day 0 (4 hours before infection), and then on Days 1, 2, and 3. Body weight loss triggered by virus infection (A, B), viral load in lung tissue (C) and nasal tissue (D), and neutrophil accumulation in BALF (E) were evaluated. For viral load, individual data have been plotted as geometric mean. For body weight. mean ± SEM was shown. *$P < 0.05$, ***$P < 0.001$ vs H1N1-infected control.

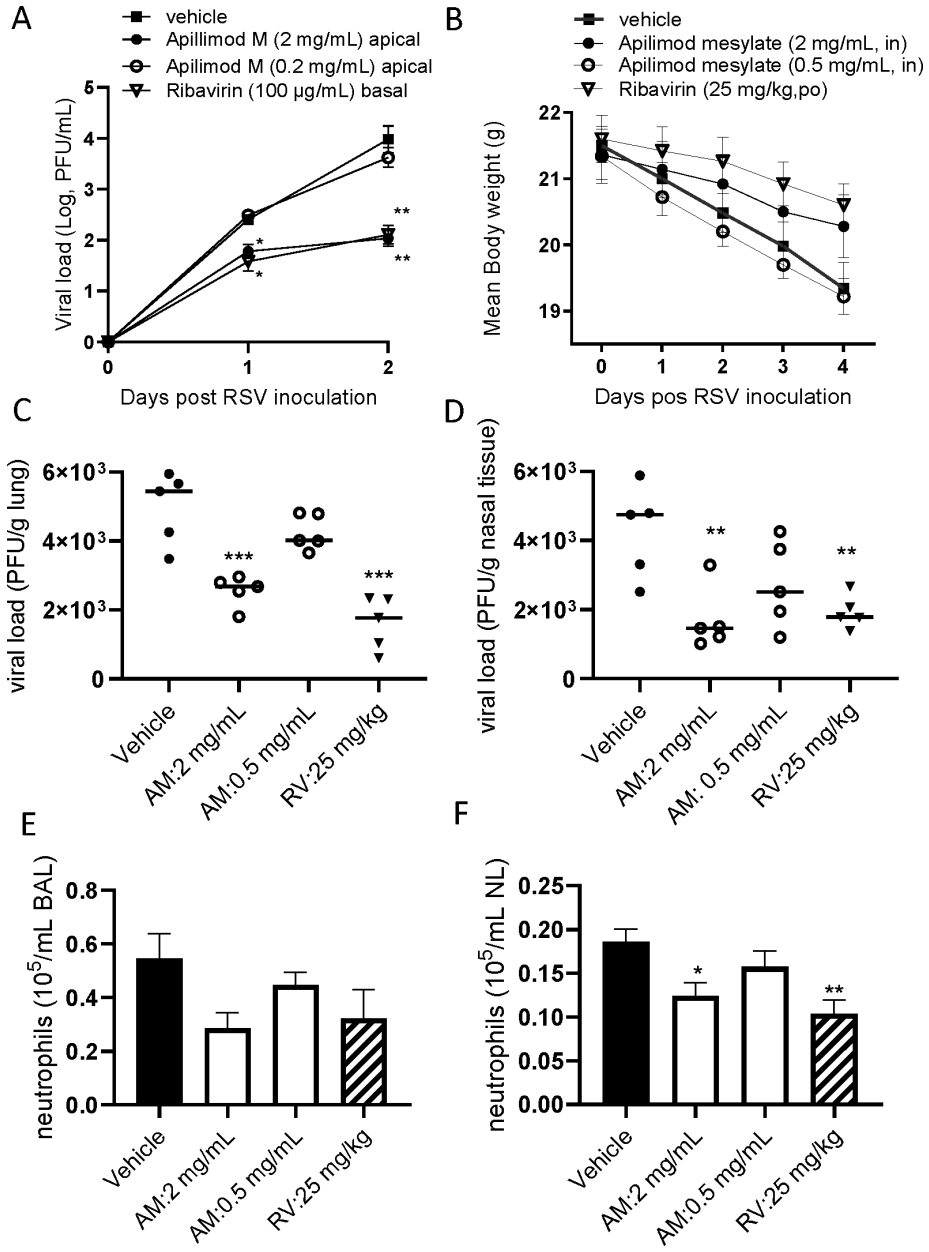

FIG 4 *In vitro* and *in vivo* antiviral effects of Apilimod against RSV infection. (A) Effects of Apilimod mesylate and ribavirin on viral load in apical washes collected from RSV A2-infected ALI-cultured nasal epithelium. Apilimod M was treated apically on Day 0 and Day 1 (and removed each time) or ribavirin was treated basally without removal. Viral load was determined by plaque assay. (B) Effects of intranasal Apilimod (Apilimod mesylate: AM) treatment on RSV A2-infected BALB/c mice. Mice were inoculated intranasally with RSV A2 (1.0×10^5 PFU/mouse), and the animals were sacrificed 4 days post-virus inoculation. AM was treated once daily on Day 0 (4 hours before infection), and then on Days 1 and 2. Body weight loss triggered by virus infection (B), viral load in lung tissue (C) and nasal tissue (D), and neutrophil accumulation in BALF (E) and nasal lavage (F) were evaluated. For viral load, individual data have been plotted and Geomean. For body weight and neutrophils, mean ± SEM were shown. *$P < 0.05$, **$P<0.01$, ***$P < 0.001$ vs RSV-infected control.

reduction) was statistically significant, which was similar to the effects of ribavirin at 100 µg/mL, treated in a basal chamber, allowing exposure for 48 hours.

Twice daily treatment with AM in mice, on days 0 to 3, by i.n. administration, was found to show beneficial effects on body weight loss triggered by virus infection where oral ribavirin at 25 mg/kg showed good protection (Fig. 4B). The viral load in the lungs

TABLE 4 Effects of Apilimod mesylate administered intranasally on H1N1-induced inflammation detected in bronchoalveolar lavage and nasal lavage of H1N1-infected mice[a]

Treatment		Cell number (mean ± SD, x10^4, [%inhibition])			Cell number (mean ± SD, [% inhibition])		
		Bronchoalveolar lavage			Nasal lavage		
	N	Neutrophils	Alveolar macrophage	Lymphocyte	Neutrophils	Alveolar macrophage	Lymphocyte
Experiment 1							
Vehicle (1% DMSO saline) + virus	5	7.9 ± 1.2	36 ± 7.0	7.3 ± 0.94	2.2 ± 0.48	5.1 ± 0.49	1.8 ± 0.14
AB (0.5 mg/mL, in) + virus	5	6.8 ± 1.5	36 ± 4.7	6.1 ± 0.42[b]	2.0 ± 0.48	4.4 ± 0.35	2.0 ± 0.30
		[14]	[0]	[16]	[9]	[14]	[−11]
AB (2 mg/mL, in) + virus	5	4.9 ± 0.76[c]	26 ± 3.3[b]	5.4 ± 0.87[c]	1.2 ± 0.38[c]	4.0 ± 0.56[c]	1.3 ± 0.10[c]
		[38]	[28]	[26]	[45]	[22]	[28]
Oseltamivir (10 mg/kg, po)	5	2.0 ± 0.96[d]	11 ± 4.3[d]	2.0 ± 0.71[d]	1.2 ± 0.38[c]	3.8 ± 0.53[c]	1.3 ± 0.30[c]
		[75]	[69]	[73]	[45]	[25]	[28]
Experiment 2							
Vehicle (water) + virus	4	7.5 ± 1.6	38 ± 3.9	7.5 ± 1.3	2.1 ± 0.57	4.7 ± 1.1	1.8 ± 0.18
AM (2 mg/mL, in) + virus	4	4.7 ± 0.91[b]	25 ± 4.8[b]	5.1 ± 1.1[b]	1.1 ± 0.38[b]	3.9 ± 0.76	1.1 ± 0.18[b]
		[37]	[34]	[32]	[48]	[17]	[39]
Experiment 3							
Vehicle (water) + virus	4	8.3 ± 2.5	40 ± 3.6	8.1 ± 1.6	2.2 ± 0.58	5.2 ± 1.0	1.8 ± 0.32
AM (2 mg/mL, in) + virus	4	6.2 ± 0.86[b]	24 ± 4.8[c]	5.0 ± 0.66[b]	1.0 ± 0.23[c]	3.6 ± 0.38[b]	0.93 ± 0.21[c]
		[25]	[40]	[38]	[55]	[31]	[48]

[a]AB: Apilimod base, AM: Apilimod mesylate, BAL: bronchoalveolar lavage, NL: nasal lavage, For experiment 1, changes in each group were compared to virus-infected animals treated with vehicle using Dunnett's one-way analysis of variance.*$P < 0.05$, **$P < 0.01$, , ***$P < 0.001$, For experiment 2 and 3, changes in each group were compared to respective vehicle control infected animals using un-paired *t*-test followed by Mann-Whitney test.
[b]$P < 0.05$.
[c]$P < 0.01$.
[d]$P < 0.001$.

and nasal tissue of RSV A2 infected BALB/c mice were significantly inhibited by 2 mg/mL intranasal AM, effects were similar to that of oral ribavirin at 25 mg/kg (Fig. 4C and D). The AM treatment also inhibited neutrophil accumulation in bronchoalveolar and nasal lavage, but the effects of AM were statistically significant only in nasal lavage (Fig. 4E and F).

DISCUSSION

Considerable efforts to identify the antiviral agents to the recent pandemic COVID-19 were made since it was outbroken, and further works have continued to develop pan-viral agents to prepare next potential pandemic. In this manuscript, we demonstrated that Apilimod is one of the promising pan-antiviral agents to tackle several respiratory virus infections.

First, Apilimod (base or mesylate [water soluble form]) inhibited replication of several influenza strains including Oseltamivir/Amantadine-resistant isolates in MDCK cells *in vitro* (Table 1; Fig. 1). These data suggest that Apilimod potentially inhibits influenza species broadly. YM, another PIKfive inhibitor, also inhibited viral replication, and therefore this appears to be a class effect. However, we found some differences in the antiviral profile between Apilimod and YM. For example, YM did not work on influenza B at the concentrations tested (21.4 µM non-toxic), although it is still inconclusive until higher concentrations of YM are tested. YM is a pyridofuropyrimidine compound with a morpholino-pyrimidine core, which has been identified in a screen for PI3K (phosphatidylinositol-3 kinase) class IA inhibitors (27). YM is a potent PIKfyve inhibitor but also has a PI3K p110α inhibitory activity (27). By contrast. Apilimod is found to be a more selective PIKfyve inhibitor without inhibitory activities against other lipid kinases (7). In addition, YM and PI-103 (a YM analog and PI3K inhibitor) are also found to be potent human two-pore channel (TPC2) blockers although Apilimod does not have the same effect (28). Thus, these compounds have strong PIKfyve activities but have different characteristics,

and the difference might affect the antiviral profile although it is still speculation. Based on the specificity, the following experiments (ALI epithelium and *in vivo*) were conducted with Apilimod.

Human influenza can infect and replicate in a number of animal species used for pre-clinical evaluation (29) and most work of this nature is conducted in mice or in ferrets. The inbred mouse strains are characterized as "semi-permissive" for the replication of human respiratory viruses, and viral replication and associated symptoms were more marked in ferrets (30). Therefore, we used H1N1 PR8, which is relatively adapted to mice. In addition, as clinical trials of oral Apilimod demonstrated limited systemic exposure, intra-nasal treatment was used to achieve appropriate concentrations locally. As demonstrated in this study, topical administration of Apilimod to the lungs through nostrils produced profound inhibition of virus production in the lung and nasal tissue and exhibited a dose-dependent steep inhibition curve in H1N1 infected BALB/c mice (Fig. 3).

The human respiratory virus is semi-permissive to animals in most cases and the outcome of non-respiratory cancer cell lines or animal cell lines is not translational. Instead, ALI-cultured airway epithelium is being increasingly recognized for its ability to overcome many of the disadvantages of submerged cell culture models (16–18) as described in the Introduction section, and, therefore, ALI-cultured primary airway cells are often used as a respiratory virus infection model (31, 32). The cellular layer consists of ciliated cells and some goblet cells, and the system shows apical shedding of progeny virions that are subsequently spread by the coordinated motion of the beating cilia, mimicking human influenza infection (33, 34). In fact, the addition of influenza at a low level of infectious particles (0.01 MOI) apically to ALI nasal epithelium, resulted in a robust, persistent infection that generated amplified viral concentrations over 7 days (Fig. 2E, and unpublished data). In addition, virus replication kinetics observed in ALI airway epithelium are similar to the outcomes from human challenge studies with SARS-CoV-2, influenza, and RSV (23–26). We were also able to translate ALI outcome (efficacy and dose) to human clinical trials (24, 35) for RSV infection. Even more importantly, we can use different treatment routes to mimic intranasal/inhaled and oral/intravenous systemic treatment using ALI two-chamber systems. In this ALI system, Apilimod displayed a concentration-dependent inhibition of influenza replication determined by $TCID_{50}$ assay following daily apical exposure (mimicking a topical/aerosol delivery to the respiratory tract) on Day 0 and Day 1 post-inoculation.

A highly desirable feature of inhaled medicines is an extended longer duration of action, thereby ensuring that therapeutic activity is maintained throughout the dosing interval. The persistence of action of Apilimod was not fully investigated, but at least once daily treatment retains effective antiviral activity in both ALI cultured fully differentiated nasal epithelium *in vitro,* as well as in mice *in vivo* (Fig. 2 and 3C). The observed persistence of the effect of Apilimod may be particularly valuable in the context of the potential use of Apilimod in prophylaxis.

Apilimod did not show strong antiviral effects against RSV A2 in the African green monkey cell line, but it demonstrated marked antiviral effects *in vitro* ALI human nasal epithelium and also mouse *in vivo*. The African green monkey cell line might be not suitable to evaluate a PIKfyve inhibitor due to toxicity. From our results with human primary nasal epithelium, the antiviral effect of Apilimod was confirmed in influenza and RSV, which are negative-sense single-stranded RNA viruses. Even more importantly, Apilimod also showed antiviral effects against positive-strand RNA viruses, such as HRV and CoV. Particularly, the effects of seasonal CoV were marked. Apilimod was also reported to show a very potent antiviral activity against SARS-CoV-2 infection in Vero cells and confirmed in Calu3 and primary lung tissue (15) although Dittmer et al. found the antiviral effects of Apilimod to be weaker in Calu3 cells compared to Vero cells (36). We preliminarily found that Apilimod also inhibited viral load in CoV229E and HRV16-infected nasal epithelium (personal communication). Further studies with different virus

species should be tested in ALI airway epithelium to prove a pan-antiviral profile of Apilimod.

Thus, Apilimod demonstrated promising antiviral potentials in this study, but there are some limitations for interpretation. First, we have not tested other animal species. Mouse has some drawbacks, especially for influenza infection due to antiviral MX-1 protein mutation (37). Ferrets for influenza and cotton rats for RSV would be preferred systems to test the effects of Apilimod in the future, although we already evaluated the antiviral effects against H1N1 and RSV in human cells using translational ALI human nasal epithelium. Secondarily, we only tested the PR8 influenza strain, largely adapted to mice, in ALI epithelium and mice. As we observed the efficacy of Apilimod against other human influenza isolates (Table 1), the animal and ALI studies with recent human influenza clinical isolates should be conducted in the future. For example, H5N1 Duck/MN/1525/81 is less pathogenic, and more clinically relevant or highly pathogenic isolates such as H5N1 2344b (38) should be tested *in vitro* and also *in vivo*. Third, we need to test with ALI epithelium from several donors, as donor-donor variation is not negligible in general in this primary cell system. In fact, previously, we reported to require, at least, four different donors to show statistically significant antiviral effects of compounds in the RSV infection system in ALI epithelium based on power calculation (24, 39). However, to resolve the issue partially, we used 13 different donor-pooled ALI-nasal epithelium in this study, provided by Epithelix. Fourth, although an advantage of pan-viral agents targeting host cell factors would be a limited development of resistant mutants, we have not evaluated the emergence of resistant mutants in this system yet. At least we confirmed Apilimod did not induce resistant variants up to 8 passages in 229E coronavirus-infected MRC5 human fibroblast cells where Nirmatrelvir-induced mutants after five passages (data not shown). Finally, a PIKfyve inhibitor potentially inhibits virus antigen presentation due to inhibition of endosome systems (40), which potentially inhibits antigen-specific T-cell activation *in vivo*. Therefore, treatment of Apilimod after virus infection is established might block antiviral immune responses. However, in the current study, we designed experiments for prophylaxis or early intervention and also experimental period is too short to determine the antiviral-antibody level. Thus, an impact of treatment on immune response should be explored in appropriately designed experiments in the future.

In summary, we found Apilimod as a potential host-directed pan-viral small-molecule inhibitor against respiratory viruses including influenza and RSV in ALI human epithelium *in vitro* and *in vivo* mouse and also against seasonal CoV and HRV *in vitro*, which constitutes a promising candidate for the treatment of respiratory virus infection in humans via intranasal delivery.

MATERIALS AND METHODS

Materials

Apilimod base, Apilimod mesylate, YM201636, oseltamivir phosphate, and oseltamivir carboxylate were purchased from MedChemExpress LLC (Monmouth Junction, NJ), ribavirin were purchased (confirmed by Pharmidex).

Cells and virus

MDCK (ATCC CCL-34) and human larynx epithelial (HEp-2) cells (ATCC CCL-23) were purchased from the American Type Culture Collection (ATCC, Manassas, VA) and maintained in 10% fetal bovine serum (FBS) supplemented DMEM with phenol red (# 4190-094: Life Technologies Ltd, Paisley, UK) at 37°C/5% CO_2. MucilAir pooled donor nasal epithelium was provided as 24-well plate sized inserts by Epithelix Sàrl (Geneva, Switzerland). Twice weekly, MucilAir inserts were transferred to a new 24-well plate containing 780 µL of MucilAir culture medium (EP04MM), and once weekly the apical surface was washed once with 400 µL PBS. MucilAir cultures were incubated at 37°C,

5% CO_2. RSV A2 Strain (#0709161v, NCPV, Public Health England, Wiltshire, UK or ATCC VR-1540) and influenza PR8 (ATCC VR-95) were propagated in HEp-2 and MDCK cells, respectively, for in-house *in vitro* work.

Antiviral panel screening

The effects of Apilimod mesylate and YM201636 against a panel of viruses were evaluated at the Institute for Antiviral Research in Utah State University. The assays were conducted as follows: Plaque reduction assay (5 days) in HEp-2 cells for RSV A (Long strain), CPE (6 days) in LLC-MK2 7.1 cells for Parainfluenza (PIV3 C243 strain), CPE (10 days) in MRC5 cells for Measles virus (Edmonton strain), CPE (5 days) in A549 cells for Influenza A virus (A/PR/34 strain), CPE (3 days) in HeLa cells for human Rhinovirus (HRV16 strain), CPE (5 days) in CEM-SS cells for HIV-1(IIIB strain), CPE (4 days) in Vero cells for Herpes Simplex Virus-1 (HF strain), and GT1b replicon luciferase assays (3 days) in Huh-7 cells for HCV.

H1N1 or RSV infection and treatment on ALI-cultured nasal epithelium

For the first H1N1 infection study, on the day of infection ("Day 0"), the apical surface of each insert was washed once with 300 µL of sterile PBS and the inserts were then transferred to new 24-well plates containing 780 µL of fresh MucilAir culture medium (Epithelix Sarl. Switzerland). PR8 virus stock was diluted in MucilAir culture medium to give a final inoculation concentration of 4,000 PFU in 100 µL (an approximate MOI of 0.02) for influenza and incubated onto cells for 1 hour at 34°C, 5% CO_2. Virus inoculum was removed with a pipette and inserts were washed twice with 300 µL of sterile media. A Day 0 sample was harvested by adding 200 µL of culture media to the apical surface of each well for 10 minutes. The 200 µL sample was then removed and transferred to 0.5 mL tubes and the tubes were stored at −80°C. This harvesting procedure was repeated daily. Transepithelial electrical resistance (TEER) was measured to investigate the integrity of tight junction dynamics in air-liquid interface-cultured pseudostratified epithelium before and after influenza infection as a surrogate for epithelial damage. Chopstick electrodes were placed in the apical and basolateral chambers and the TEER was measured using a dedicated volt-ohm meter (EVOM2, Epithelial Volt/Ohm Meter for TEER) and expressed as Ohm/cm^2. 50 µL of compound solution was applied on Day 0, and incubated for 10 min, and virus inoculum was applied on top of the treatment for 1 hour. On Day 1, 50 µL of compound solution was applied, incubated for 15 min, and then removed. Oseltamivir was applied in a basolateral chamber 10 min before virus inoculation, and it was applied again on Day 1. Viral load was assessed by $TCID_{50}$ assay.

For the second H1N1 study shown in Table 3 and RSV A2 study, 50 µL of the compound solution or PBS was carefully applied to the apical site and incubated at 37°C/5% CO_2 for 15 min. H1N1 PR8 virus or RSV A2 virus stock was diluted in MucilAir culture medium to give a final inoculation concentration of 4,000 PFU in 50 µL, and applied to the apical site on top of the treatment (2,000 PFU in final, approximately an MOI of 0.01). Cells were incubated for another hour at 37°C/5% CO_2, and then the apical media including virus inoculum was carefully removed with a pipette. After the apical wash twice with PBS, the third apical wash was collected as Day 0 sample. Apical wash from the RSV study was collected in 12.5% sucrose solution (final concentration). On Day 1 (next day), 300 µL of warm PBS was applied to the apical surface, and after 5 min, the first wash was collected for viral load. Following the first wash, 50 µL of compound solution or PBS was applied to the apical surface and removed after 30 min incubation. On Day 2, 300 µL of warm PBS was applied to the apical surface, and after 5 min, the first wash was collected daily for viral load assessment by plaque assay. Oseltamivir carboxylate or ribavirin was also applied to a basal chamber for the H1N1 and RSV A2 study, respectively.

In vivo H1N1 infection

BALB/c mice (male, 20–30 g) were inoculated intranasally on Day 0 with H1N1 PR8 (0.65×10^5 PFU/mouse) in Pharmidex UK. Animals were sacrificed 3 days after the inoculation, and bronchoalveolar lavage and nasal lavage were collected for inflammation. The lungs and nasal tissue were also collected for the preparation of tissue homogenate. Apilimod base (Santa Cruz Biotechnolgy, Heidelberg, Germany) was prepared as a suspension in 10% DMSO/90% isotonic saline and delivered using an intranasal installation of 40 µL/mouse at doses of 0.5, or 2 mg/mL on Day −1, again on Day 0 (1 hour before inoculation) and then once daily on Days 1, 2, and 3 post-inoculations. Apilimod mesylate was also prepared as a solution in sterile water and treated intranasally. Oseltamivir phosphate (Sigma-Aldrich) was suspended in PBS and was administered by oral gavage (10 mL/kg). Viral load was determined by plaque assay using MDCK cells in the presence of L-1-tosylamido-2-phenylethyl chloromethyl ketone (TPCK)-treated trypsin 1.0 µg/mL, and the plaque was detected by crystal violet staining 3 days after inoculation. The detection limit was 50 PFU/mL of tissue homogenate. Viral load was corrected to the weight of lung homogenate and shown as PFU/g tissue. All animal works were reviewed by the internal AWERB (Animal Welfare Ethical Review) committee in Pharmidex Ltd. and have been conducted under the United Kingdom home office project license PP0969406.

In vivo RSV infection

BALB/c mice (male, 20–30 g) were inoculated intranasally on Day 0 with RSV A2 (0.65×10^5 PFU/mouse) in Pharmidex UK. Animals were sacrificed 4 days after the inoculation, and the lungs were collected for preparation of lung homogenate. Apilimod base was prepared as a suspension in 10% DMSO/90% isotonic saline and delivered using an intratracheal installation of 20 µL/mouse or intranasal installation of 40 µL/mouse at doses of 0.2, or 2 mg/mL on Day −1, again on Day 0 (1 hour before inoculation) and then once daily on Days 1, 2, and 3 post-inoculations. All animal works were reviewed by the internal AWERB (Animal Welfare Ethical Review) committee in Pharmidex Ltd. and have been conducted under the United Kingdom home office project license PP0969406.

$TCID_{50}$ assay for H1N1

Serial dilutions of the apical wash samples with media containing 0.1 µg/mL TPCK Trypsin were applied to plate wells containing an 80% confluency of MDCK cells and incubated at 35°C with 5% CO_2 for 3–5 days until the cytopathic effects of vehicle control became visible. $TCID_{50}$ was calculated using the Reed-Muench formula (41).

Plaque assay for H1N1

Serial dilutions of the apical wash samples from ALI culture or mouse lavage samples were applied to plate wells containing an 80% confluency of MDCK cells. The inoculated cells were incubated at 37°C with 5% CO_2 for 1 hour after which the inoculum was removed from the wells and the cells washed (twice) with PBS before applying an overlay of 1% methylcellulose agar media (including growth media plus TPCK trypsin) to each well. Once the agar media had been set, the plates were placed in an incubator at 37°C with 5% CO_2 for 3 days after which the resulting plaques will counted. A second count was conducted once the agar had been removed by fixing and staining the cells with crystal violet. Data were presented as mean ± sem of pfu for each group.

Plaque assay for RSV

HEp2 cells were grown in 24-well plates prior to infection in DMEM containing 10% vol/vol FBS until they attained 100% confluency. Apical wash samples from ALI culture were thawed out at room temperature and serial dilutions were prepared in serum-free DMEM. The growth medium from HEp2 cells was aspirated and replaced with 300 µL of serially diluted lung/nasal tissue homogenate (along with stock RSV-only

positive control) or ALI culture apical wash, and left to infect at 37°C/5% CO_2 for 4 hours. The infectious media was then aspirated and replaced with 500 µL Plaque Assay Overlay (1% wt/vol methylcellulose in MEM, 2% vol/vol FBS, 1% wt/vol pen/strep, 0.5 µg/mL amphotericin B), and left for 7 days at 37°C/5% CO_2. Cells were fixed with ice-cold methanol for 10 minutes after which they were washed twice with sterile PBS. Anti-RSV F-protein antibody [2F7] was diluted to a 1:150 concentration in blocking buffer (5% wt/vol powdered milk (Marvel) in 0.05% vol/vol PBS-Tween 20) and 150 µL was added to cells for 2 hours at room temperature with shaking. Cells were washed 2× using PBS before 150 µL of secondary antibody (goat anti-mouse/HRP conjugate) diluted 1:400 in blocking buffer were added to cells for 1 hour at room temperature, with shaking. The secondary antibody solution was removed, and cells were washed twice with PBS. 150 µL of the metal-enhanced development substrate DAB prepared in ultra-pure water was applied to the cells until plaques were visible. Plaques were counted by eye and confirmed using light microscopy, allowing the calculation of plaque-forming units per mL.

Lactose dehydrogenase Assay

Lactose dehydrogenase (LDH) concentrations of collected samples were measured using a commercial ELISA kit (Abcam, UK) as per the manufacturer's instructions. Optical density was measured at 450 nM using a microplate reader (SpectraMax 340PC). Concentrations of LDH were determined using SoftMax Pro v. 6.4 (Molecular Devices).

Statistical analysis

Results were represented as mean ± standard error of the mean. The $IC_{50,}$ IC_{90}, and CC_{50} values were calculated using GraphPad Prism (GraphPad Software Inc., La Jolla, CA). The safety index was calculated as the ratio of the CC_{50} and IC_{50} values. Multiple comparison was performed by ANOVA followed by Dunnett's multiple comparison test performed using the PRISM 6 software program. If no significance was achieved using ANOVA analysis, non-parametric Kruskal-Wallis analysis followed by Dunn's multiple comparison test was conducted. The comparison between the two groups was performed by unpaired *t*-test with Welch's correction or Mann-Whitney test. Statistical significance was defined as $P < 0.05$.

ACKNOWLEDGMENTS

We thank Jag Shur, SubIntro Ltd. for the insightful discussion.

This study was supported by SubIntro Ltd (London, UK).

K.I., G.R., and J.B. conceived and designed the experiments. J.B., H.O., L.D., and I.K. performed the experiments. The first draft of the manuscript was written by K.I. All authors contributed to the technical interpretation, the interpretation of the result, and the editing of the manuscript.

AUTHOR AFFILIATIONS

[1]National Heart and Lung Institute, Imperial College, London, United Kingdom
[2]Pharmidex, London, United Kingdom

PRESENT ADDRESS

Jonathan Baker, King's College, London, United Kingdom

AUTHOR ORCIDs

Kazuhiro Ito http://orcid.org/0000-0001-9320-2717

FUNDING

Funder	Grant(s)	Author(s)
SubIntro Ltd.		Jonathan Baker
		Hugo Ombredane

AUTHOR CONTRIBUTIONS

Jonathan Baker, Conceptualization, Data curation, Formal analysis, Funding acquisition, Writing – review and editing | Hugo Ombredane, Investigation, Methodology, Writing – review and editing | Leah Daly, Funding acquisition, Investigation, Writing – review and editing | Ian Knowles, Formal analysis, Investigation, Methodology, Writing – review and editing | Garth Rapeport, Conceptualization, Writing – review and editing | Kazuhiro Ito, Conceptualization, Data curation, Formal analysis, Supervision, Writing – original draft

DATA AVAILABILITY

Data will be available on request.

REFERENCES

1. Linden D, Guo-Parke H, Coyle PV, Fairley D, McAuley DF, Taggart CC, Kidney J. 2019. Respiratory viral infection: a potential "missing link" in the pathogenesis of COPD. Eur Respir Rev 28:180063. https://doi.org/10.1183/16000617.0063-2018
2. Zheng X-Y, Xu Y-J, Guan W-J, Lin L-F. 2018. Regional, age and respiratory-secretion-specific prevalence of respiratory viruses associated with asthma exacerbation: a literature review. Arch Virol 163:845–853. https://doi.org/10.1007/s00705-017-3700-y
3. Cookson W, Moffatt M, Rapeport G, Quint J. 2022. A pandemic lesson for global lung diseases: exacerbations are preventable. Am J Respir Crit Care Med 205:1271–1280. https://doi.org/10.1164/rccm.202110-2389CI
4. Jin Y, Deng Z, Zhu T. 2022. Membrane protein trafficking in the anti-tumor immune response: work of endosomal-lysosomal system. Cancer Cell Int 22:413. https://doi.org/10.1186/s12935-022-02805-6
5. Yong X, Mao L, Shen X, Zhang Z, Billadeau DD, Jia D. 2021. Targeting endosomal recycling pathways by bacterial and viral pathogens. Front Cell Dev Biol 9:648024. https://doi.org/10.3389/fcell.2021.648024
6. Nelson EA, Dyall J, Hoenen T, Barnes AB, Zhou H, Liang JY, Michelotti J, Dewey WH, DeWald LE, Bennett RS, Morris PJ, Guha R, Klumpp-Thomas C, McKnight C, Chen Y-C, Xu X, Wang A, Hughes E, Martin S, Thomas C, Jahrling PB, Hensley LE, Olinger GG, White JM. 2017. The phosphatidylinositol-3-phosphate 5-kinase inhibitor apilimod blocks filoviral entry and infection. PLoS Negl Trop Dis 11:e0005540. https://doi.org/10.1371/journal.pntd.0005540
7. Cai X, Xu Y, Cheung AK, Tomlinson RC, Alcázar-Román A, Murphy L, Billich A, Zhang B, Feng Y, Klumpp M, Rondeau J-M, Fazal AN, Wilson CJ, Myer V, Joberty G, Bouwmeester T, Labow MA, Finan PM, Porter JA, Ploegh HL, Baird D, De Camilli P, Tallarico JA, Huang Q. 2013. PIKfyve, a class III PI kinase, is the target of the small molecular IL-12/IL-23 inhibitor apilimod and a player in Toll-like receptor signaling. Chem Biol 20:912–921. https://doi.org/10.1016/j.chembiol.2013.05.010
8. Wada Y, Cardinale I, Khatcherian A, Chu J, Kantor AB, Gottlieb AB, Tatsuta N, Jacobson E, Barsoum J, Krueger JG. 2012. Apilimod inhibits the production of IL-12 and IL-23 and reduces dendritic cell infiltration in psoriasis. PLoS One 7:e35069. https://doi.org/10.1371/journal.pone.0035069
9. Krausz S, Boumans MJH, Gerlag DM, Lufkin J, van Kuijk AWR, Bakker A, de Boer M, Lodde BM, Reedquist KA, Jacobson EW, O'Meara M, Tak PP. 2012. Brief report: a phase IIa, randomized, double-blind, placebo-controlled trial of apilimod mesylate, an interleukin-12/interleukin-23 inhibitor, in patients with rheumatoid arthritis. Arthritis Rheum 64:1750–1755. https://doi.org/10.1002/art.34339
10. Sands BE, Jacobson EW, Sylwestrowicz T, Younes Z, Dryden G, Fedorak R, Greenbloom S. 2010. Randomized, double-blind, placebo-controlled trial of the oral interleukin-12/23 inhibitor apilimod mesylate for treatment of active Crohn's disease. Inflamm Bowel Dis 16:1209–1218. https://doi.org/10.1002/ibd.21159
11. Kang Y-L, Chou Y-Y, Rothlauf PW, Liu Z, Soh TK, Cureton D, Case JB, Chen RE, Diamond MS, Whelan SPJ, Kirchhausen T. 2020. Inhibition of PIKfyve kinase prevents infection by Zaire ebolavirus and SARS-CoV-2. Proc Natl Acad Sci U S A 117:20803–20813. https://doi.org/10.1101/2020.04.21.053058
12. Kumar P, Mathayan M, Smieszek SP, Przychodzen BP, Koprivica V, Birznieks G, Polymeropoulos MH, Prabhakar BS. 2022. Identification of potential COVID-19 treatment compounds which inhibit SARS Cov2 prototypic, Delta and Omicron variant infection. Virology 572:64–71. https://doi.org/10.1016/j.virol.2022.05.004
13. Kettunen P, Lesnikova A, Räsänen N, Ojha R, Palmunen L, Laakso M, Lehtonen Š, Kuusisto J, Pietiläinen O, Saber SH, Joensuu M, Vapalahti OP, Koistinaho J, Rolova T, Balistreri G. 2023. SARS-CoV-2 infection of human neurons is TMPRSS2 independent, requires endosomal cell entry, and can be blocked by inhibitors of host phosphoinositol-5 kinase. J Virol 97:e0014423. https://doi.org/10.1128/jvi.00144-23
14. Luo Z, Liang Y, Tian M, Ruan Z, Su R, Shereen MA, Yin J, Wu K, Guo J, Zhang Q, Li Y, Wu J. 2023. Inhibition of PIKFYVE kinase interferes ESCRT pathway to suppress RNA virus replication. J Med Virol 95:e28527. https://doi.org/10.1002/jmv.28527
15. Riva L, Yuan S, Yin X, Martin-Sancho L, Matsunaga N, Burgstaller-Muehlbacher S, Pache L, De Jesus PP, Hull MV, Chang M, et al. 2020. A large-scale drug repositioning survey for SARS-CoV-2 antivirals. bioRxiv. https://doi.org/10.1101/2020.04.16.044016
16. Zarkoob H, Allué-Guardia A, Chen Y-C, Jung O, Garcia-Vilanova A, Song MJ, Park J-G, Oladunni F, Miller J, Tung Y-T, Kosik I, Schultz D, Yewdell J, Torrelles JB, Martinez-Sobrido L, Cherry S, Ferrer M, Lee EM. 2021. Modeling SARS-CoV-2 and influenza infections and antiviral treatments in human lung epithelial tissue equivalents. bioRxiv:2021.05.11.443693. https://doi.org/10.1101/2021.05.11.443693
17. Baldassi D, Gabold B, Merkel O. 2021. Air-liquid interface cultures of the healthy and diseased human respiratory tract: promises, challenges and future directions. Adv Nanobiomed Res 1:2000111. https://doi.org/10.1002/anbr.202000111
18. Michi AN, Proud D. 2021. A toolbox for studying respiratory viral infections using air-liquid interface cultures of human airway epithelial cells. Am J Physiol Lung Cell Mol Physiol 321:L263–L280. https://doi.org/10.1152/ajplung.00141.2021
19. Liu J, Cao R, Xu M, Wang X, Zhang H, Hu H, Li Y, Hu Z, Zhong W, Wang M. 2020. Hydroxychloroquine, a less toxic derivative of chloroquine, is effective in inhibiting SARS-CoV-2 infection *in vitro*. Cell Discov 6:16. https://doi.org/10.1038/s41421-020-0156-0
20. Cochin M, Touret F, Driouich J-S, Moureau G, Petit P-R, Laprie C, Solas C, de Lamballerie X, Nougairède A. 2022. Hydroxychloroquine and

azithromycin used alone or combined are not effective against SARS-CoV-2 *ex vivo* and in a hamster model. Antiviral Res 197:105212. https://doi.org/10.1016/j.antiviral.2021.105212
21. Deng J, Zhou F, Heybati K, Ali S, Zuo QK, Hou W, Dhivagaran T, Ramaraju HB, Chang O, Wong CY, Silver Z. 2021. Efficacy of chloroquine and hydroxychloroquine for the treatment of hospitalized COVID-19 patients: a meta-analysis. Future Virol. https://doi.org/10.2217/fvl-2021-0119
22. Maisonnasse P, Guedj J, Contreras V, Behillil S, Solas C, Marlin R, Naninck T, Pizzorno A, Lemaitre J, Gonçalves A, Kahlaoui N, Terrier O, Fang RHT, Enouf V, Dereuddre-Bosquet N, Brisebarre A, Touret F, Chapon C, Hoen B, Lina B, Calatrava MR, van der Werf S, de Lamballerie X, Le Grand R. 2020. Hydroxychloroquine use against SARS-CoV-2 infection in non-human primates. Nature 585:584–587. https://doi.org/10.1038/s41586-020-2558-4
23. Killingley B, Mann AJ, Kalinova M, Boyers A, Goonawardane N, Zhou J, Lindsell K, Hare SS, Brown J, Frise R, et al. 2022. Safety, tolerability and viral kinetics during SARS-CoV-2 human challenge in young adults. Nat Med 28:1031–1041. https://doi.org/10.1038/s41591-022-01780-9
24. Brookes DW, Coates M, Allen H, Daly L, Constant S, Huang S, Hows M, Davis A, Cass L, Ayrton J, Knowles I, Strong P, Rapeport G, Ito K. 2018. Late therapeutic intervention with a respiratory syncytial virus L-protein polymerase inhibitor, PC786, on respiratory syncytial virus infection in human airway epithelium. Br J Pharmacol 175:2520–2534. https://doi.org/10.1111/bph.14221
25. DeVincenzo J, Cass L, Murray A, Woodward K, Meals E, Coates M, Daly L, Wheeler V, Mori J, Brindley C, Davis A, McCurdy M, Ito K, Murray B, Strong P, Rapeport G. 2022. Safety and antiviral effects of nebulized PC786 in a respiratory syncytial virus challenge study. J Infect Dis 225:2087–2096. https://doi.org/10.1093/infdis/jiaa716
26. Han A, Czajkowski LM, Donaldson A, Baus HA, Reed SM, Athota RS, Bristol T, Rosas LA, Cervantes-Medina A, Taubenberger JK, Memoli MJ. 2019. A dose-finding study of a wild-type influenza A(H3N2) virus in a healthy volunteer human challenge model. Clin Infect Dis 69:2082–2090. https://doi.org/10.1093/cid/ciz141
27. Jefferies HBJ, Cooke FT, Jat P, Boucheron C, Koizumi T, Hayakawa M, Kaizawa H, Ohishi T, Workman P, Waterfield MD, Parker PJ. 2008. A selective PIKfyve inhibitor blocks PtdIns(3,5)P(2) production and disrupts endomembrane transport and retroviral budding. EMBO Rep 9:164–170. https://doi.org/10.1038/sj.embor.7401155
28. Du C, Guan X, Yan J. 2022. Two-pore channel blockade by phosphoinositide kinase inhibitors YM201636 and PI-103 determined by a histidine residue near pore-entrance. Commun Biol 5:738. https://doi.org/10.1038/s42003-022-03701-5
29. Bem RA, Domachowske JB, Rosenberg HF. 2011. Animal models of human respiratory syncytial virus disease. Am J Physiol Lung Cell Mol Physiol 301:L148–L156. https://doi.org/10.1152/ajplung.00065.2011
30. Nguyen T-Q, Rollon R, Choi Y-K. 2021. Animal models for influenza research: strengths and weaknesses. Viruses 13:1011. https://doi.org/10.3390/v13061011
31. Liu X, Wu Y, Rong L. 2020. Conditionally reprogrammed human normal airway epithelial cells at ALI: a physiological model for emerging viruses. Virol Sin 35:280–289. https://doi.org/10.1007/s12250-020-00244-z
32. Heinen N, Klöhn M, Steinmann E, Pfaender S. 2021. *In vitro* lung models and their application to study SARS-CoV-2 pathogenesis and disease. Viruses 13:792. https://doi.org/10.3390/v13050792
33. Zhang L, Peeples ME, Boucher RC, Collins PL, Pickles RJ. 2002. Respiratory syncytial virus infection of human airway epithelial cells is polarized, specific to ciliated cells, and without obvious cytopathology. J Virol 76:5654–5666. https://doi.org/10.1128/jvi.76.11.5654-5666.2002
34. Villenave R, Shields MD, Power UF. 2013. Respiratory syncytial virus interaction with human airway epithelium. Trends Microbiol 21:238–244. https://doi.org/10.1016/j.tim.2013.02.004
35. DeVincenzo JP, McClure MW, Symons JA, Fathi H, Westland C, Chanda S, Lambkin-Williams R, Smith P, Zhang Q, Beigelman L, Blatt LM, Fry J. 2015. Activity of oral ALS-008176 in a respiratory syncytial virus challenge study. N Engl J Med 373:2048–2058. https://doi.org/10.1056/NEJMoa1413275
36. Dittmar M, Lee JS, Whig K, Segrist E, Li M, Kamalia B, Castellana L, Ayyanathan K, Cardenas-Diaz FL, Morrisey EE, Truitt R, Yang W, Jurado K, Samby K, Ramage H, Schultz DC, Cherry S. 2021. Drug repurposing screens reveal cell-type-specific entry pathways and FDA-approved drugs active against SARS-Cov-2. Cell Rep 35:108959. https://doi.org/10.1016/j.celrep.2021.108959
37. Staeheli P, Grob R, Meier E, Sutcliffe JG, Haller O. 1988. Influenza virus-susceptible mice carry Mx genes with a large deletion or a nonsense mutation. Mol Cell Biol 8:4518–4523. https://doi.org/10.1128/mcb.8.10.4518-4523.1988
38. Duriez O, Sassi Y, Le Gall-Ladevèze C, Giraud L, Straughan R, Dauverné L, Terras A, Boulinier T, Choquet R, Van De Wiele A, Hirschinger J, Guérin J-L, Le Loc'h G. 2023. Highly pathogenic avian influenza affects vultures' movements and breeding output. Curr Biol 33:3766–3774. https://doi.org/10.1016/j.cub.2023.07.061
39. Ito K, Daly L, Coates M. 2023. An impact of age on respiratory syncytial virus infection in air-liquid-interface culture bronchial epithelium. Front Med (Lausanne) 10:1144050. https://doi.org/10.3389/fmed.2023.1144050
40. Baranov MV, Bianchi F, van den Bogaart G. 2020. The PIKfyve inhibitor apilimod: a double-edged sword against COVID-19. Cells 10:30. https://doi.org/10.3390/cells10010030
41. Bullen CK, Davis SL, Looney MM. 2022. Quantification of infectious SARS-CoV-2 by the 50% tissue culture infectious dose endpoint dilution assay. Methods Mol Biol 2452:131–146. https://doi.org/10.1007/978-1-0716-2111-0_9